cally separate ventricles that allow the complete separation of systemic and pulmonary circulations. However, shunting blood away from the lungs and into the systemic circulation is possible in the crocodilian heart because the right ventricle gives rise not only to the pulmonary arteries but also to another major vessel, the left aorta (Fig. 2a). This allows deoxygenated right-ventricular blood to bypass the lungs and to be re-circulated into the systemic circulation (pulmonary-to-systemic shunt) — that is, blood is ejected into the left aorta instead of the pulmonary arteries. For a pulmonary-to-systemic shunt to develop, the pressure in the right ventricle must exceed the pressure in the left aorta[4–8].

The cog-teeth[1–3] connective tissue nodules (Fig. 2a, b) are one of the intriguing anatomical features of the crocodilian heart. They project from the subpulmonary conus into the pulmonary outflow tract just proximal to the pulmonary leaf-like valves and fit snugly together during systole, reducing the diameter of the subpulmonary conus[3]. Indirect evidence[9–12], such as the spontaneous appearance of a biphasic pressure peak in the right ventricle, suggests that the cog-teeth might be an 'extra' valve mechanism that could help in initiating and regulating shunts.

We used a crocodile heart preparation[6] perfused *in situ* to determine the function and possible regulation of this valve. The perfused heart generated a cardiac output similar to that recorded *in vivo* and worked at physiological pressures. Using an antagonist of the β-adrenergic receptor, sotalol, we initiated a shunt where about a third of the output from the right ventricle exited through the left aorta. Injecting adrenaline or isoprenaline into the right side of the heart reduced flow to the left aorta and eventually abolished the shunt, with flow being redirected into the pulmonary artery (Fig. 2c). This indicated that control of the shunt within the heart of *C. porosus* was mediated by an intrinsic β-adrenoceptor.

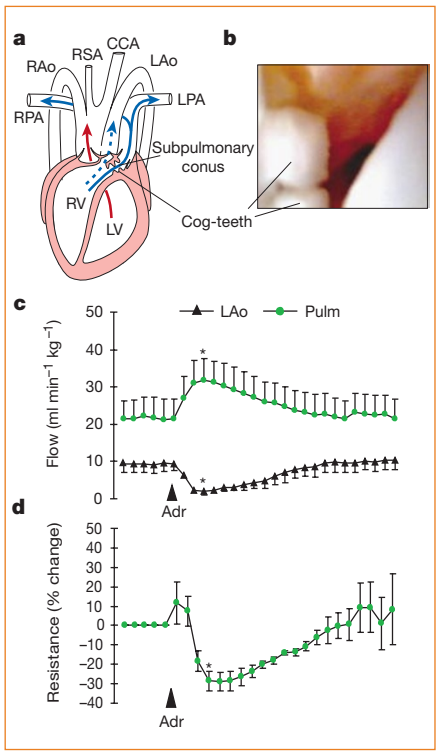

Figure 2 The 'cog-teeth' valve inside the heart of crocodilians and the flow and resistance from a perfused *Crocodylus porosus* heart preparation[6]. **a,** The crocodilian heart, outflow tract and major arteries, showing the position of the cog-teeth within the subpulmonary conus, proximal to the leaflet pulmonary valves and surrounded by cardiac muscle. During non-shunting conditions, blood is ejected from the left ventricle (LV) into the right aorta (RAo) (leading to the dorsal aorta), right subclavian artery (RSA) and the common carotid artery (CCA) (red arrow). The right ventricle (RV) ejects blood into the common pulmonary trunk which divides into the left and right pulmonary arteries (LPA and RPA) (blue arrow). During shunting, blood is ejected from the right ventricle into the left aorta (LAo) (dotted arrow). **b,** Angioscopic image[3] of the 'cog-teeth' in the subpulmonary conus in the right ventricle; pointers show individual cogs. Photo courtesy of C. Löfman. **c,** The effect of a bolus injection of adrenaline (Adr, 0.3 ml 10^{-7} M) on pulmonary and left aortic flows, and **d,** on pulmonary outflow resistance, in a *C. porosus* perfused-heart preparation pretreated with the β-adrenoceptor-antagonist sotalol. Sotalol induced a shunt in the perfused heart preparation, despite the left-aortic output pressure being set at 1.5 kPa above the pulmonary artery output pressure. A bolus injection of adrenaline eliminated the shunt, with flow in the left aorta being diverted back into the pulmonary outflow tract. The bolus injection of adrenaline resulted in a significant reduction (28.9 ± 4.9%) in pulmonary outflow resistance (means ± s.e.m.; $n = 6$; asterisks indicate a significant difference at $P < 0.05$, Wilcoxon signed rank test).

Neither heart rate nor the total power output generated by the heart preparation changed during the injection of adrenaline/isoprenaline, excluding the possibilities that the shunt was mediated by a change in the inotropic state of the heart or as the result of a change in stroke volume (Starling effect). The shunt induced by sotalol was the result of a large increase in resistance of the pulmonary outflow tract. The injected boluses of adrenaline and isoprenaline decreased the resistance of the pulmonary outflow tract, corresponding to the increased flow in the pulmonary artery (Fig. 2d). As the effects of the bolus injections wore off, the resistance of the pulmonary tract increased again and the shunt returned.

Our results demonstrate the presence and action of a regulatory intra-cardiac valve within the subpulmonary conus of the estuarine crocodile and indicate that the initiation of a shunt occurs when the β-adrenergic drive on the heart is low.

Craig E. Franklin*, Michael Axelsson†
**Department of Zoology and Entomology, University of Queensland, Brisbane, Queensland 4072, Australia*
e-mail: cfranklin@zen.uq.edu.au
†Department of Zoophysiology, University of Göteborg, PO Box 463, Göteborg 405 30, Sweden

1. van Mierop, L. H. S. & Kutsche, L. M. in *Cardiovascular Shunts: Phylogenetic, Ontogenetic and Clinical Aspects* (Munksgaard, Copenhagen, 1985).
2. Webb, G. J. W. *J. Morphol.* **161,** 221–240 (1979).
3. Axelsson, M., Franklin, C. E., Löfman, C. O., Nilsson, S. & Grigg, G. C. *J. Exp. Biol.* **199,** 359–365 (1996).
4. Grigg, G. C. & Johansen, K. *J. Comp. Physiol.* **157,** 381–392 (1987).
5. Shelton, G. & Jones, D. R. *J. Exp. Biol.* **158,** 539–564 (1991).
6. Franklin, C. E. & Axelsson, M. *J. Exp. Biol.* **186,** 269–288 (1994).
7. Axelsson, M., Nilsson, S. & Holm, S. *Am. J. Physiol.* **256,** R875–R879 (1989).
8. Malvin, G. M., Hicks, J. W. & Green, R. E. *Am. J. Physiol.* **269,** R1133–R1139 (1995).
9. White, F. *Copeia* **3,** 567–570 (1969).
10. Greenfield, L. J. & Morrow, A. G. *J. Surg. Res.* **1,** 97–103 (1961).
11. White, F. N. *Am. Zool.* **8,** 211–219 (1968).
12. Jones, D. R. & Shelton, G. *J. Exp. Biol.* **176,** 247–269 (1993).

FRANK LANE PICTURE AGENCY/CORBIS

Figure 1 The estuarine crocodile *Crocodylus porosus* has an unusual valve inside its heart that can shunt blood away from the lungs.

Erratum

A triclosan-resistant bacterial enzyme
Richard J. Heath, Charles O. Rock
Nature **406,** 145–146 (2000)
In Table 1, the third entry should have been *Streptococcus pneumoniae*, and not *Salmonella pneumoniae* as published.

vol. 8 (ed. Waterman, P. G.) 51–131 (Academic, New York, 1993).
6. Nahrstedt, A. & Davis, R. H. *Comp. Biochem. Physiol.* **75B,** 65–73 (1983).
7. Raubenheimer, D. *J. Chem. Ecol.* **15,** 2177–2189 (1989).
8. Chamberlain, P. & MacKenzie, R. M. in *Cyanide in Biology* (eds Vennesland, B., Conn, E. E., Knowles, C. J., Westley, J. & Wissing, F.) 184–196 (Academic, New York, 1981).
9. Conn, E. E. in *Cyanide in Biology* (eds Vennesland, B., Conn, E. E., Knowles, C. J., Westley, J. & Wissing, F.) 335–348 (Academic, New York, 1981).
10. Adsersen, A., Brimer, L., Olsen, C. E. & Jaroszewski, J. W. *Phytochemistry* **33,** 365–367 (1993).

Microbiology

A triclosan-resistant bacterial enzyme

Triclosan is an antimicrobial agent that is widely used in a variety of consumer products and acts by inhibiting one of the highly conserved enzymes (enoyl-ACP reductase, or FabI) of bacterial fatty-acid biosynthesis. But several key pathogenic bacteria do not possess FabI, and here we describe a unique triclosan-resistant flavoprotein, FabK, that can also catalyse this reaction in *Streptococcus pneumoniae*. Our finding has implications for the development of FabI-specific inhibitors as antibacterial agents.

FabI from *Escherichia coli* catalyses the reduction of enoyl-ACP during each cycle of fatty-acid elongation[1,2] and is inhibited by triclosan[3–6]; InhA, the enoyl-ACP reductase from mycobacteria, is the target for the antituberculosis drug isoniazid[7]. Both drugs block the same essential step in bacterial fatty-acid synthesis. But the *fabI* gene is conspicuously absent from several bacterial genomes (Table 1) and as enoyl-ACP reduction is essential for survival, organisms lacking FabI must have a different gene to encode enoyl-ACP reductase.

We have investigated the reductase reaction in *S. pneumoniae*, in which the entire set of *fab* genes, except *fabI*, is present in a cluster spanning 10 kilobases of the genome (GenBank accession number, AF197933). A similar *fab* gene cluster was found in the clostridia. Subsets of the *fab* genes are clustered in the genomes of other bacteria, but individual genes are also sprinkled throughout the genome[1]. We found that there is one unidentified open reading frame, termed *fabK*, predicted to encode a 34K protein (FabK), within the streptococcal and clostridial *fab* clusters. The predicted protein had a centrally located FAD-binding domain[8] (FAD is a flavin-linked redox cofactor).

We purified the FabK protein and found that it contained 0.8 molecules of FAD per FabK monomer. The protein had a specific activity of 66 ± 4 nmol min^{-1} mg^{-1} in an *in vitro* enoyl-ACP reductase coupled-assay system, in which purified *E. coli* Fab proteins generated the *trans*-2-butenoyl-ACP substrate (Fig. 1). Another cofactor, NADH, was essential for enoyl-ACP reductase activity and FabK was able slowly to oxidize NADH, but not NADPH, in the absence of substrate. *In vitro*, FabK activity was more than 100-fold more resistant to triclosan than was FabI.

We transformed *E. coli* strain RJH13 (which harbours a temperature-sensitive allele (*fabI*(ts)) and fails to grow at 42 °C)[2] with a plasmid that constitutively expresses FabK and found that growth was restored at the non-permissive temperature, indicating that FabK substitutes for all of the functions of FabI.

The wild-type *E. coli* strain W3110 is sensitive to triclosan (Table 1), and overexpression of FabI and the chromosomal *fabI*[G93V] mutant could each increase resistance to triclosan 8- to 64-fold[4]. Introduction of the FabK expression vector into strain W3110 shifted the minimum inhibitory concentration (MIC) for triclosan by more than 4 orders of magnitude up to over 2,000 μg ml^{-1}. The marked resistance of these cells to triclosan confirms that FabK is not a target for triclosan and that FabI is the only triclosan target in *E. coli*.

In some bacteria, FabI is not the only target for triclosan. Organisms that contain only *fabI* are highly susceptible to triclosan (MIC < 0.5 mg ml^{-1}), whereas those carrying *fabK* are uniformly more resistant (> 2 mg ml^{-1}) (Table 1). The discovery of a triclosan-resistant enoyl-ACP reductase (FabK) in *S. pneumoniae* demonstrates that a triclosan target other than enoyl-ACP reductase is responsible for the sensitivity of this Gram-positive organism to the drug. Among Gram-negative bacteria, *Pseudomonas aeruginosa* is unique in that it not only contains both *fabI* and *fabK* in its genome but is also refractory to triclosan (Table 1). This is due in part to possession of a mechanism for active efflux of the drug[9]; however, disruption of the triclosan-sensitive *fabI* gene does not result in a growth phenotype, and enoyl-ACP activity in extracts of the *fabI*-null strain is resistant to inhibition by triclosan[10]. Thus, *P. aeruginosa* must contain a second, triclosan-resistant enoyl reductase, which we suggest may be a FabK homologue.

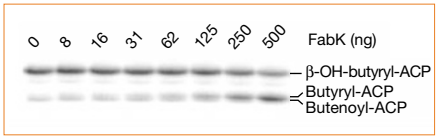

Figure 1 FabK is an enoyl-ACP reductase. Histidine-tagged FabK protein from *S. pneumoniae* was expressed in *E. coli* strain BL21-Codon Plus-(DE3)-R1L (Stratagene) and purified by metal-chelation affinity chromatography. A coupled enzyme system[11] was used to assay FabK by combining all the purified *E. coli* proteins required to reconstitute a cycle of fatty-acid synthesis, apart from enoyl-ACP reductase. A reaction mixture containing 100 μM ACP, 1 mM β-mercaptoethanol, 100 μM acetyl-CoA, 50 μM [2-^{14}C]malonyl-CoA (56 mCi $mmol^{-1}$), 200 μM NADPH, 200 μM NADH and 12.5 μg ml^{-1} each of FabD, FabH, FabG, FabA and FabZ in 0.1 M sodium phosphate, pH 7.0, was incubated at 37 °C for 30 min to generate the *trans*-2-enoyl-ACP substrate before being aliquoted into individual tubes, to which FabK was added to the amount indicated and incubated for 30 min at 37 °C. Products were separated by conformationally sensitive gel electrophoresis; bands were stained and their intensity quantified by using a PhosphorImager.

The discovery of a unique enoyl-ACP reductase has important implications for antibacterial drug development. Organisms expressing FabK are predicted to be refractory to inhibitors designed to target FabI. Conversely, selective FabK inhibitors would be effective against several important pathogens, such as the streptococci and clostridia. Organisms such as the pseudomonads and enterococci that contain both a FabI and FabK will require a combination of enoyl-ACP reductase inhibitors to block growth. Thus, antimicrobial therapy based on blocking enoyl-ACP reductase will need to be tailored for specific pathogens according to their expression of FabI and FabK.

Table 1 **Distribution and triclosan sensitivity of FabI and FabK in bacteria**

Organism	*Sequence identity (%)**		*Triclosan MIC†*
	FabI	*FabK*	*(μg ml^{-1})*
Escherichia coli	100	—	0.25
Staphylococcus aureus	43	—	0.01
Salmonella pneumoniae	—	100	2.0
Clostridium acetobutylicum	—	58	3.0
Enterococcus faecalis	47	68	10
Mycobacterium tuberculosis	33	31	100
Pseudomonas aeruginosa	69	33	> 1,000

Dashes indicate that no homologous genes were detected.
*Identity to FabI and FabK is shown. FabI homologues are easily recognized in both Gram-negative and Gram-positive bacterial genomes by using BLAST search algorithms, but these are not present in several pathogens. The *E. coli* FabI and *S. pneumoniae* FabK protein sequences were used to search the unfinished and complete database of microbial genomes (see http://www.tigr.org) for open reading frames encoding homologous proteins, and the number of identical residues was scored.
†Minimum inhibitory concentration (MIC) values are from ref. 12.

Richard J. Heath*, Charles O. Rock*†
**Department of Biochemistry, St Jude Children's Research Hospital, Memphis, Tennessee 38105, USA*
†Department of Biochemistry, University of Tennessee, Memphis, Tennessee 38105, USA
e-mail: charles.rock@stjude.org

1. Rock, C. O. & Cronan, J. E. Jr *Biochim. Biophys. Acta* **1302,** 1–16 (1996).
2. Heath, R. J. & Rock, C. O. *J. Biol. Chem.* **270,** 26538–26542 (1995).

3. McMurray, L. M., Oethinger, M. & Levy, S. *Nature* **394,** 531–532 (1998).
4. Heath, R. J. *et al. J. Biol. Chem.* **273,** 30316–30321 (1998).
5. Heath, R. J. *et al. J. Biol. Chem.* **274,** 11110–11114 (1999).
6. Levy, C. W. *et al. Nature* **398,** 383–384 (1999).
7. Rozwarski, D., Grant, G., Barton, D., Jacobs, W. & Sacchettini, J. C. *Science* **279,** 98–102 (1998).
8. Nagy, M., Lacroute, F. & Thomas, D. *Proc. Natl Acad. Sci. USA* **89,** 8966–8970 (1992).
9. Schweizer, H. P. *Antimicrob. Agents Chemother.* **42,** 394–398 (1998).
10. Hoang, T. T. & Schweizer, H. P. *J. Bacteriol.* **181,** 5489–5497 (1999).
11. Heath, R. J. & Rock, C. O. *J. Biol. Chem.* **271,** 1833–1836 (1996).
12. Bhargava, H. N. & Leonard, P. A. *Am. J. Infect. Control* **24,** 209–218 (1996).

Materials science

Diffusion of a polymer 'pancake'

Thread-like chains of flexible polymers that adsorb to a solid surface assume a flat 'pancake' conformation[1] when the surface coverage is low and are only able to diffuse in two dimensions because so many segments are adsorbed. Here we show that the centre-of-mass diffusion coefficient of the polymer chain, measured at dilute coverage to ensure minimal chain–chain interaction, has a strong power-law dependence on the degree of polymerization. This nonlinear dependence of polymer diffusion on a solid surface contrasts with the linear dependence observed on a fluid membrane[2].

Our system consisted of polyethylene glycol (PEG) adsorbed from aqueous solution onto a monolayer surface of self-assembled octadecyltriethoxysilane[3] coated onto a fused silica coverslip to render it hydrophobic (because PEG does not adsorb from aqueous solution to hydrophilic fused silica at high pH).

Diffusion was investigated by fluctuation correlation spectroscopy[4–6] of a mono-end-labelled fluorescent probe after two-photon excitation. The focused two-photon beam creates an illuminated spot with a beam waist of about 0.3 μm. The small number of fluorophores contained within a given volume (typically 3–10) fluctuates as polymers diffuse in and out. The fit to the autocorrelation function determines the mutual diffusion coefficient (D_M) of the fluorescing species, and $D_M \approx D$, the centre-of-mass diffusion coefficient, because the system is dilute. Experiments were followed using a Zeiss microscope with a 63× Plan Apochromat objective (numerical aperture 1.4).

We varied the PEG polymer chain length (Fig. 1 legend) by a factor of 15. Polymers were allowed to adsorb for less than 5 min from dilute (1–10 nM) solution in 0.01 M aqueous phosphate buffer, pH 8.4. To study bulk solutions, PEG samples were labelled with fluorescein 5-isothiocyanate, and for monitoring surface diffusion, we used an Alexa-488 label (from Molecular Probes), a derivatized rhodamine-green molecule. Control experiments demonstrated that unattached fluorescent labels did not adsorb, confirming that adsorption was controlled by polymer–surface attraction. At this dilute surface coverage, 0.5–2% of the saturating amount of polymer adsorbed.

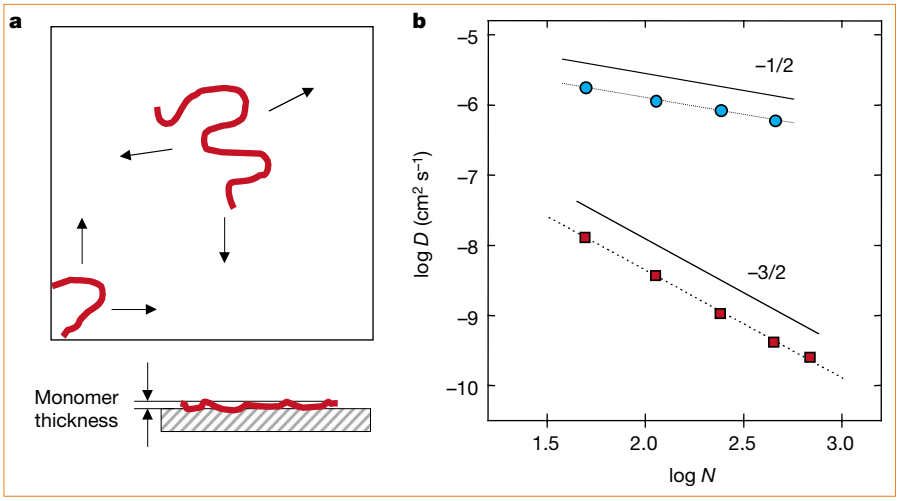

Figure 1 Comparison of polymer diffusion when adsorbed to a solid surface and in free solution. **a,** Flexible polymer chains that adsorb are nearly flat at dilute surface coverage ('de Gennes pancake'). The sticking energy for each segment is small, so no single segment is bound tightly, but the molecular sticking energy is large. **b,** Diffusion coefficients (D) in dilute solution (circles) and at dilute coverage on a solid surface (squares) are plotted on log–log scales against degree of polymerization (N) at 22 °C, for chains of weight-average molecular weights, M_w, of 2,200, 5,000, 10,800, 20,100 and 30,500 g-mol^{-1} and M_w/M_n values of 1.01–1.03 (where M_n is the number-average molecular weight).

We estimated the 'sticking energy' of the polymer as 0.5–1 k_BT per segment, where k_B is Boltzmann's constant at T the absolute temperature. This emerged consistently from analysis of the Langmuir isotherm at low surface coverage, and from Arrhenius analyses of the very slow desorption rate and of the data presented below after extrapolation to the molecular weight of a single segment. Polymer chains thus adsorb, at low coverage, in a flat 'pancake' conformation[1] (Fig. 1a).

Measurements of D (Fig. 1b) reveal a power-law scaling with the number of chain segments (N), so $D \approx N^{-3/2}$. This is strikingly stronger than the $D \approx N^{-1}$ relation observed for charged, semi-flexible DNA obeying excluded volume statistics but adsorbed by Coulombic attraction on a fluid lipid membrane[2]. The key difference is that adsorption sites on a solid surface are static, so the rate-limiting events concern the polymer rather than surface. For diffusion in solution, our results are consistent with standard hydrodynamic results for chains of moderate length, when $D \approx N^{-1/2}$ (refs 7,8).

Reptation (the diffusion of a chain, snakelike, along its own length) may explain this stronger dependence of D on N for polymers under our conditions. In this model[1], the terminal relaxation time scales as $\tau_{rept} \approx N^3$. Knowing that the radius of gyration (R_g) scales as $R_g \approx N^{3/4}$ in a good solvent in two dimensions[2,9], and arguing that $D \approx R_g^2/\tau_{rept}$, it follows that $D \approx N^{-3/2}$ for chains with excluded-volume statistics, as we find here. A simulation for a single self-avoiding chain diffusing among regularly spaced obstacles in two dimensions also gives $D \approx N^{-3/2}$ (ref. 10). But interpreting the value of scaling exponents is a problem, particularly as they seem to depend on obstacle density[11].

Reptation may be considered surprising in a dilute system where the physical origin of the static constraints that suppress lateral motion is unclear. But if there were some slack between sticking points — for example, loops of an isolated flexible chain might propagate with high probability along its length in a caterpillar-like fashion — the mathematics of the reptation model would then apply, despite the unconventional physical situation.

Svetlana A. Sukhishvili*, Yan Chen†, Joachim D. Müller†, Enrico Gratton†, Kenneth S. Schweizer*, Steve Granick*

**Department of Materials Science and Engineering, University of Illinois, Urbana, Illinois 61801, USA*
†Laboratory for Fluorescence Dynamics, Department of Physics, University of Illinois, Urbana, Ilinois 61801, USA

1. de Gennes, P.-G. *Scaling Concepts in Polymer Physics* (Cornell Univ. Press, Ithaca, NY, 1979).
2. Maier, B. & Rädler, O. *Phys. Rev. Lett.* **82,** 1911–1914 (1999).
3. Kessel, C. R. & Granick, S. *Langmuir* **7,** 532–538 (1991).
4. Magde, D., Elson, E. L. & Webb, W. W. *Biopolymers* **13,** 29–61 (1974).
5. Berland, K. M., So, P. T. C. & Gratton, E. *Biophys. J.* **68,** 694–701 (1995).
6. So, P. T. C. *et al. Bioimaging* **3,** 1–15 (1995).
7. Yuko, K. & Chikako, H. *Polym. Commun.* **25,** 154–157 (1984).
8. Huber, K., Bantle, S., Lutz, P. & Burchard, W. *Macromolecules* **18,** 1461–1467 (1985).
9. des Cloizeaux, J. & Jannink, G. *Polymers in Solution* (Clarendon, Oxford, 1990).
10. Azuma, R. & Takayama, H. *J. Chem. Phys.* **111,** 8666–8671 (1999).
11. Slater, G. W. & Wu, S. Y. *Phys. Rev. Lett.* **75,** 164–168 (1995).